marine drugs

MDPI

Article

New Prenylated Indole Homodimeric and Pteridine Alkaloids from the Marine-Derived Fungus *Aspergillus austroafricanus* Y32-2

Peihai Li [1,2,3,†], Mengqi Zhang [1,2,3,†], Haonan Li [1], Rongchun Wang [1,3], Hairong Hou [1,3], Xiaobin Li [1,3,*], Kechun Liu [1,3,*] and Hao Chen [4,*]

1 Engineering Research Center of Zebrafish Models for Human Diseases and Drug Screening of Shandong Province, Shandong Provincial Engineering Laboratory for Biological Testing Technology, Biology Institute, Qilu University of Technology (Shandong Academy of Sciences), Jinan 250103, China; liph@sdas.org (P.L.); mengqi@sdas.org (M.Z.); 17862958363@163.com (H.L.); wangrc@sdas.org (R.W.); houhr@sdas.org (H.H.)
2 State Key Laboratory of Biobased Material and Green Papermaking, Qilu University of Technology (Shandong Academy of Sciences), Jinan 250353, China
3 Key Laboratory for Biosensor of Shandong Province, Biology Institute, Qilu University of Technology (Shandong Academy of Sciences), Jinan 250103, China
4 Key Laboratory of Marine Bioactive Substances, First Institute of Oceanography, Ministry of Natural Resources, Qingdao 266061, China
* Correspondence: lixb@sdas.org (X.L.); hliukch@sdas.org (K.L.); hchen@fio.org.cn (H.C.); Tel./Fax: +86-531-82605352 (X.L.); +86-531-82605331 (K.L.); +86-532-88963855 (H.C.)
† These authors contributed equally to this work.

Abstract: Chemical investigation of secondary metabolites from the marine-derived fungus *Aspergillus austroafricanus* Y32-2 resulted in the isolation of two new prenylated indole alkaloid homodimers, di-6-hydroxydeoxybrevianamide E (**1**) and dinotoamide J (**2**), one new pteridine alkaloid asperpteridinate A (**3**), with eleven known compounds (**4**–**14**). Their structures were elucidated by various spectroscopic methods including HRESIMS and NMR, while their absolute configurations were determined by ECD calculations. Each compound was evaluated for pro-angiogenic, anti-inflammatory effects in zebrafish models and cytotoxicity for HepG2 human liver carcinoma cells. As a result, compounds **2**, **4**, **5**, **7**, **10** exhibited pro-angiogenic activity in a PTK787-induced vascular injury zebrafish model in a dose-dependent manner, compounds **7**, **8**, **10**, **11** displayed anti-inflammatory activity in a $CuSO_4$-induced zebrafish inflammation model, and compound **6** showed significant cytotoxicity against HepG2 cells with an IC_{50} value of 30 μg/mL.

Keywords: marine-derived fungus; *Aspergillus austroafricanus*; novel bioactive metabolites; pro-angiogenesis; anti-inflammatory effects

Citation: Li, P.; Zhang, M.; Li, H.; Wang, R.; Hou, H.; Li, X.; Liu, K.; Chen, H. New Prenylated Indole Homodimeric and Pteridine Alkaloids from the Marine-Derived Fungus *Aspergillus austroafricanus* Y32-2. *Mar. Drugs* **2021**, *19*, 98. https://doi.org/10.3390/md19020098

Academic Editor: Asunción Barbero
Received: 16 January 2021
Accepted: 5 February 2021
Published: 9 February 2021

1. Introduction

The ocean has the characteristics of high salinity, high pressure, low temperature, low oxygen content, and oligotrophic environment, which enables microorganisms to have unique metabolic adaptation mechanisms and produce natural products with novel structures and diverse bioactivities [1]. Marine-derived fungi have been found to be a rich source of natural products due to their complex genetic background and abundant metabolites [2]. In recent years, a large number of novel secondary metabolites, such as polyketides, alkaloids, terpenes, steroids, peptides, etc., have been discovered from marine-derived *Aspergillus* species [3], and showed diverse bioactivities like antibacterial, antitumor, antioxidant, and anti-inflammatory activities [4]. More than 80% natural products were directly or indirectly related to small molecule drugs for the treatment of various diseases in the last 30 years, and many marine alkaloids with bioactivities have been comprehensively studied for drug development [5,6].

In our previous study, a series of fungal secondary metabolites were isolated and characterized with antitumor or cardiovascular effects [7,8]. To discover more natural products with pharmacological activities from marine-derived fungi, the fungal strain *Aspergillus austroafricanus* Y32-2 has been isolated from a seawater sample collected from the Indian Ocean. Chemical investigation of the secondary metabolites of Y32-2 fermented on rice medium resulted in the isolation of fourteen compounds, including two new prenylated indole alkaloid homodimers and one new pteridine alkaloid, named di-6-hydroxydeoxybrevianamide E (**1**), dinotoamide J (**2**) and asperpteridinate A (**3**), along with eleven known compounds (**4**–**14**) [7,9–16] (Figure 1). Among them, compound **4** was isolated for the first time as a natural product.

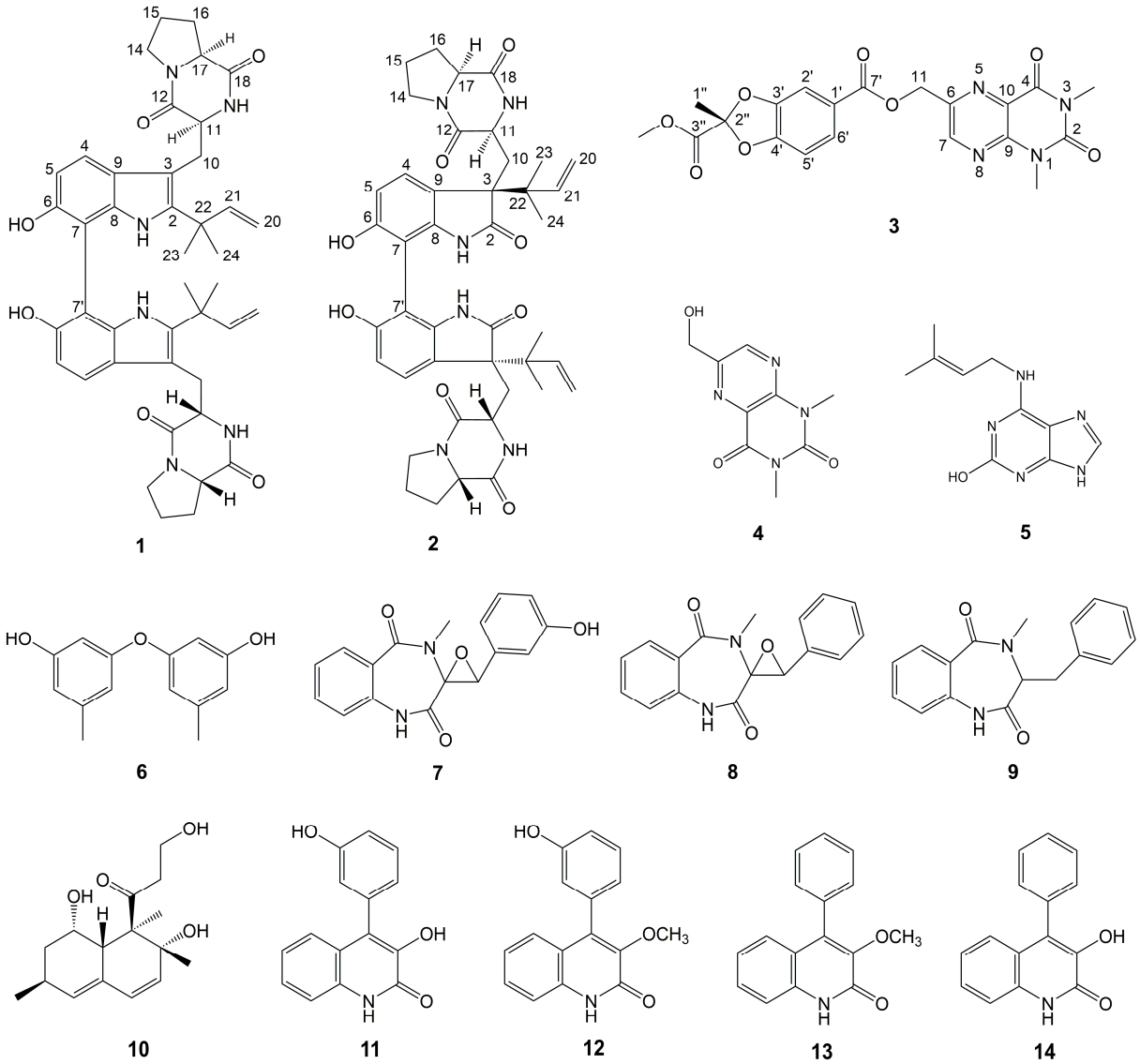

Figure 1. Structures of Compounds **1**–**14**.

The prenylated indole alkaloids contain a bicyclo[2.2.2]diazaoctane or diketopiperazine ring, and has been reported to have antitumor, antibacterial, and insecticidal activities [17]. Here two new prenylated indole alkaloid homodimers and other isolated compounds were all tested for pro-angiogenic and anti-inflammatory effects in zebrafish models and cytotoxicity towards HepG2 human liver carcinoma cells. Compounds **2**, **4**, **5**, **7**, and **10** exhibited angiogenesis promoting activity in a dose-dependent manner. Compounds **7**, **8**, **10**, and **11** also displayed anti-inflammatory activity in a dose-dependent

manner. In addition, compound **6** showed cytotoxicity against HepG2 cells. In this paper, the isolation, structure elucidation, and bioactivity of all isolated compounds are reported.

2. Results and Discussion

2.1. Structure Elucidation

Compound **1**, obtained as yellow amorphous powder, possessed a molecular formula of $C_{42}H_{48}N_6O_6$ by the negative HR-ESI-MS (*m/z* 731.3559 $[M - H]^-$, calculated 731.3557), requiring 22 unsaturations. The HPLC chromatographic behavior of **1** was unusual and existed always as a 1:1 inseparable mixture. Many of the NMR signals also appeared in pairs, hinting towards structural distinctiveness and complexity. The ^{1}H NMR spectrum (Table 1) in DMSO-d_6 of **1** showed two pairs of mutually coupled aromatic protons at δ_H 7.35, 7.37 (each H, d, J = 8.4 Hz) and 6.80, 6.81 (each H, d, J = 8.4 Hz), a set of vinyl proton signals at δ_H 6.15, 6.17 (each H, dd, J = 17.5, 10.7 Hz), 5.06 (2H, br d, J = 17.5 Hz) and 5.01 (2H, br d, J = 10.7 Hz), four methyl singlets at δ_H 1.42 (12H, s), as well as six active hydrogen signals at δ_H 9.09 (2H, br s), 8.45, 8.58 (each H, s) and 6.21, 6.30 (each H, s). The ^{13}C NMR spectrum (Table 1) showed four amidocarbonyl carbon signals at δ_C 169.3, 169.4 (C-18, 18′) and 165.6 (C-12, 12′, overlapped), twenty aromatic or olefinic carbon signals, containing four vinyl carbons at δ_C 146.4, 146.5 (C-21, 21′) and 111.29, 111.33 (C-20, 20′), and four nitrogen-bearing methine signals at δ_C 58.5 (C-17, 17′, overlapped) and 55.0, 55.3 (C-11, 11′). The above NMR features were similar to those of 6-hydroxydeoxybrevianamide E [18], a cyclic dipeptide produced by *Aspergillus* and *Penicillium* species, and a careful and rigorous analysis of the ^{1}H, ^{1}H-COSY and HMBC correlations (Figure 2) also supported this inference. However, there were two obvious differences in their NMR signals: (1) different substitution patterns on the indole ring; (2) most of the NMR signals in **1** appeared in pairs. Based on the HSQC and HMBC correlation, the C-7, 7′ (δ_C 104.0, 104.1) were aromatic quaternary carbon signals that were different from 6-hydroxydeoxybrevianamide E, confirmed that the positions C-7, 7′ of the indole ring were substituted. Considering its molecular formula, compound **1** was deduced as a dimer of 6-hydroxydeoxybrevianamide E via C-7 and C-7′. Due to a certain steric hindrance, the structure existed as a 1:1 mixture of inseparable rotamers. The relative configuration of the cyclic dipeptide moiety was determined by the NOESY correlation (Figure 2) of H-11 and H-17. Based on the relative configuration, two probable forms of its absolute configuration, 1a (11*S*, 17*S*, 11′*S*, 17′*S*) and 1b (11*R*, 17*R*, 11′*R*, 17′*R*), were respectively used for the ECD calculations, and the absolute configuration was assigned as 11*S*, 17*S*, 11′*S*, 17′*S* (Figure 3), which was in consistent with that of 6-hydroxydeoxybrevianamide E. Therefore, the structure of **1** was unequivocally established as shown in Figure 1 and named as di-6-hydroxydeoxybrevianamide E.

Table 1. 400 MHz ^{1}H and 150 MHz ^{13}C NMR data of compounds **1** and **2** in DMSO-d_6.

No.	1		2	
	δ_C Type	δ_H (Mult., J in Hz)	δ_C Type	δ_H (Mult., J in Hz)
2,2′	139.1, 139.2 C	—	180.1 C	—
3,3′	104.75, 104.82 C	—	55.9 C	—
4,4′	117.6, 117.8 CH	7.35, 7.37 (each H, d, 8.4)	126.0 CH	7.11 (2H, d, 8.2)
5,5′	109.9, 110.0 CH	6.80, 6.81 (each H, d, 8.4)	106.9 CH	6.39 (2H, d, 8.2)
6,6′	150.0, 150.1 C	—	155.7 C	—
7,7′	104.0, 104.1 C	—	104.0 C	—
8,8′	134.4, 134.5 C	—	143.4 C	—
9,9′	122.6, 122.7 C	—	118.4 C	—
10,10′	25.3, 25.4 CH_2	2.94, 3.52 (each 2H, m)	30.3 CH_2	2.03 (2H, dd, 14.7, 5.2) 2.80 (2H, dd, 14.7, 4.7)
11,11′	55.0, 55.3 CH	4.33, 4.38 (each H, dd, 9.2, 4.2)	52.6 CH	3.41 (2H, dd, 5.2, 4.7)

Table 1. *Cont.*

No.	1		2	
	δ_C Type	δ_H (Mult., *J* in Hz)	δ_C Type	δ_H (Mult., *J* in Hz)
12,12′	165.6 C	—	165.6 C	—
14,14′	44.8 CH_2	3.37, 3.47 (each 2H, m)	45.1 CH_2	3.23, 3.35 (each 2H, m)
15,15′	22.2 CH_2	1.75−1.91 (4H, m)	22.3 CH_2	1.67−1.79 (4H, m)
16,16′	27.6 CH_2	1.85, 2.12 (each 2H, m)	27.1 CH_2	1.77, 1.99 (each 2H, m)
17,17′	58.5 CH	4.22 (2H, t-like, 7.2)	58.3 CH	4.02 (2H, t-like, 7.6)
18,18′	169.3, 169.4 C	—	169.8 C	—
20,20′	111.29, 111.33 CH_2	5.01 (2H, br d, 10.7) 5.06 (2H, br d, 17.5)	112.6 CH_2	4.94 (2H, br d, 17.5) 5.00 (2H, br d, 10.9)
21,21′	146.4, 146.5 CH	6.15, 6.17 (each H, dd, 17.5, 10.7)	143.9 CH	6.15 (2H, dd, 17.5, 10.9)
22,22′	38.6, 38.7 C	—	42.2 C	—
23,23′	27.5, 27.6 CH_3	1.42 (6H, s)	21.1 CH_3	0.98 (6H, s)
24,24′	27.5, 27.6 CH_3	1.42 (6H, s)	22.6 CH_3	0.96 (6H, s)
1,1′-NH	—	8.45, 8.58 (each H, s)	—	9.31 (2H, s)
19,19′-NH	—	6.21, 6.30 (each H, s)	—	7.57 (2H, s)
6,6′-OH	—	9.09 (2H, br s)	—	9.28 (2H, br s)

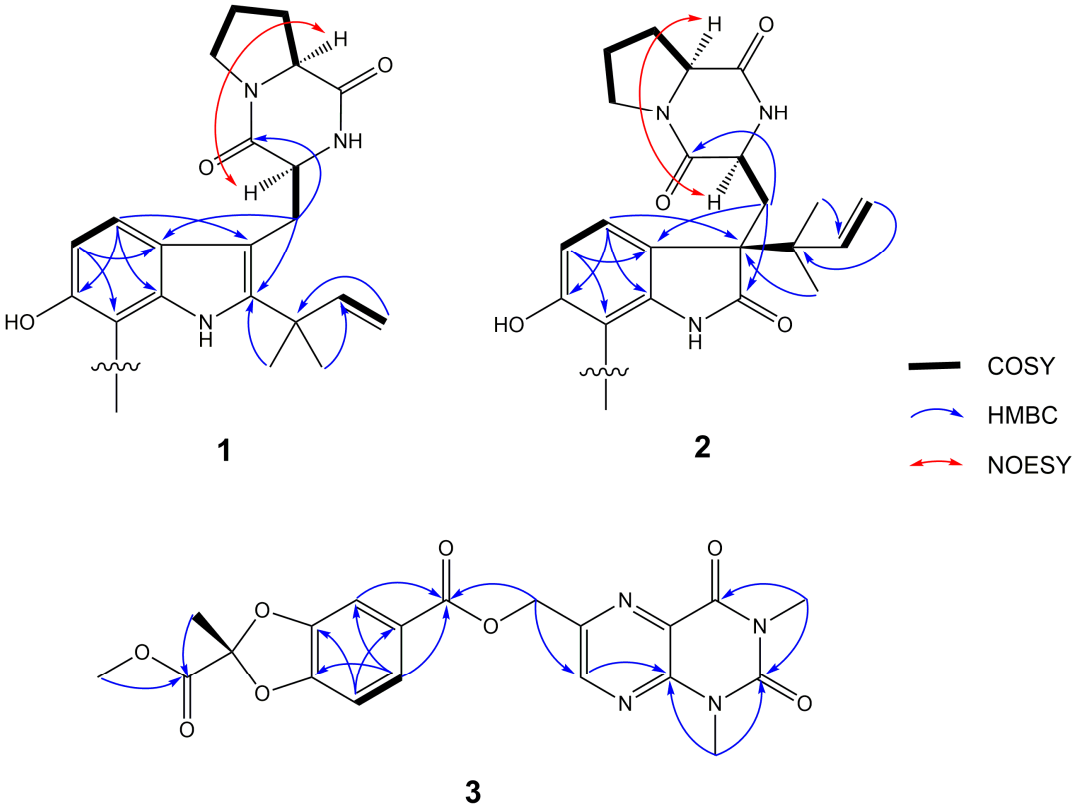

1 **2** **3**

Figure 2. The ^{1}H, ^{1}H-correlation spectroscopy (^{1}H, ^{1}H-COSY), key heteronuclear multiple-bond correlation spectroscopy (HMBC) and nuclear overhauser effect spectroscopy (NOESY) correlations of compounds **1**, **2** (only half showed) and **3**.

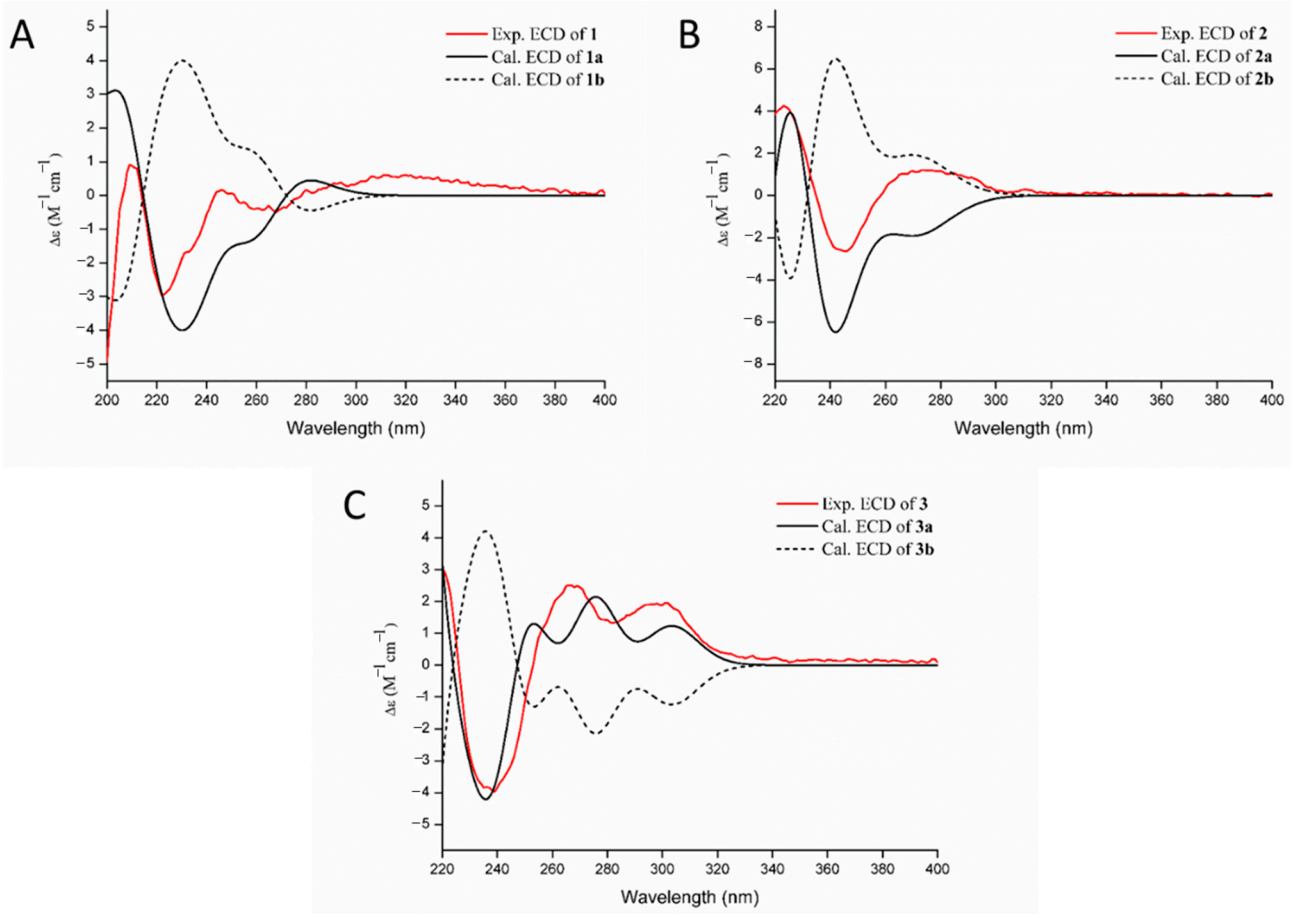

Figure 3. Measured CD and calculated equivalent circulating density (ECD) curves of compounds **1** (**A**), **2** (**B**) and **3** (**C**).

Compound **2** was obtained as a yellow amorphous powder. The molecular formula was determined to be $C_{42}H_{48}N_6O_8$ by the negative HRESIMS (*m/z* 763.3440 $[M - H]^-$, calculated 763.3456), indicating 22 degrees of unsaturation. The NMR spectra (Table 1) of **2** revealed 24 proton and 21 C-atom signals, suggesting **2** to be a symmetrical homodimer. The ^{1}H NMR spectrum for **2** showed two aromatic proton signals at δ_H 7.11 (1H, d, J = 8.2 Hz) and 6.39 (1H, d, J = 8.2 Hz), three vinyl proton signals at δ_H 4.94 (1H, br d, J = 17.5 Hz), 5.00 (1H, br d, J = 10.9 Hz) and 6.15 (1H, dd, J = 17.5, 10.9 Hz), two methyl singlets at δ_H 0.96 (3H, s), 0.98 (3H, s), as well as three active hydrogen signals at δ_H 7.57 (1H, s), 9.28 (1H, br s), and 9.31 (1H, s). The ^{13}C NMR data (Table 1) revealed the presence of three carbonyl carbon signals at δ_C 180.1 (C-2), 169.8 (C-18) and 165.6 (C-12), eight aromatic or olefinic carbon signals containing two vinyl carbons at δ_C 143.9 (C-21) and 112.6 (C-20), and two nitrogen-bearing methines at δ_C 58.3 (C-17) and 52.6 (C-11). Extensive comparison of the above NMR spectra with those of notoamide J [17] revealed that both structures were very similar, except for the substitution patterns on the C-7 position of indole ring. Considering its molecular formula, compound **2** was also identified as a homodimer of notoamide J via C-7 and C-7′. Due to one single signal set in the NMR spectrum, one single peak in the chiral column chromatography and less steric hindrance in the structure than compound **1**, it was deduced to be a freely rotating homologous dimer. With the aid of the ^{1}H, ^{1}H-COSY, HSQC and HMBC correlations, the planar structure of **2** was established as shown (Figure 1). The relative configuration of the cyclic dipeptide moiety was deduced by a NOESY correlation between H-11 and H-17, suggested that both protons had the same co-facial orientation. Because of the similar NMR data between **2** and notoamide J, the relative configuration of the positions C-3, C-11 and C-17 were determined to be similar to that of notoamide J [17]. By comparison of the experimental and calculated ECD spectra of **2**, the absolute configuration was tentatively assigned as 3*R*, 11*S*, 17*S*, 3′*R*, 11′*S*, and

17′*S* (Figure 3), which was also probably verified by the identical CD spectrum between **2** and notoamide J. So, the structure of **2** was tentatively assigned as shown in Figure 1 and named as dinotoamide J.

Asperpteridinate A was obtained as a yellow amorphous powder. The molecular formula $C_{20}H_{18}N_4O_8$ was assigned on the basis of the HRESIMS peak at m/z 465.1018 $[M + Na]^+$ (calcd. 465.1023), requiring 14 degrees of unsaturation. The ^1H NMR spectrum of **3** showed the signals for a 1,2,4-trisubstituted benzene ring system at δ_H 7.49 (1H, d, J = 1.4 Hz), 7.10 (1H, d, J = 8.3 Hz) and 7.65 (1H, dd, J = 8.3, 1.4 Hz), one vinyl proton at δ_H 8.94 (1H, s), three O-methyl or N-methyl at δ_H 3.74 (3H, s), 3.53 (3H, s), 3.31 (3H, s), one O-methylene at δ_H 5.49 (2H, s), one methyl at δ_H 1.90 (3H, s). The ^{13}C NMR data (Table 2) revealed the presence of four carbonyl at δ_C 150.6 (C-2), 159.7 (C-4), 164.8 (C-7′), 166.4 (C-3′′), ten aromatic or olefinic carbons, containing four vinyl carbons at δ_C 145.8 (C-6), 147.2 (C-7), 147.7 (C-9), 127.2 (C-10), one O-methyl at δ_C 53.5 (O-CH3), one O-methylene at δ_C 64.7 (O-CH2-). ^1H and ^{13}C NMR (Table 2) spectra analysis revealed that some signals of **3** was similar to that of compound **4** [9] and 2, 2-dimethyl-1, 3-dioxa-benzo[d]pentane-6-carboxylic acid [19]. With the aid of the ^1H, ^1H-COSY, HSQC, and HMBC correlations, the structure of **3** was established as shown (Figures 1 and 2). The absolute configuration of **3** at C-2″ was also determined as 2″*R* by ECD calculations (Figure 3).

Table 2. 400 MHz ^1H and 150 MHz ^{13}C NMR data of compound **3** in DMSO-d_6.

No.	δ_C, Type	δ_H, (Mult., *J* Hz)
2	150.6 C	—
4	159.7 C	—
6	145.8 C	—
7	147.2 CH	8.94 (1H, s)
9	147.7 C	—
10	127.2 C	—
11	64.7 CH_2	5.49 (2H, s)
1′	123.6 C	—
2′	109.2 CH	7.49 (1H, d, 1.4)
3′	147.0 C	—
4′	150.9 C	—
5′	108.8 CH	7.10 (1H, d, 8.3)
6′	125.9 CH	7.65 (1H, dd, 8.3, 1.4)
7′	164.8 C	—
1″	21.7 CH_3	1.90 (3H, s)
2″	112.6 C	—
3″	166.4 C	—
N1-Me	29.2 CH_3	3.53 (3H, s)
N3-Me	28.7 CH_3	3.31 (3H, s)
3″-OMe	53.5 CH_3	3.74 (3H, s)

2.2. Biological Activity

In previous report, some alkaloids from marine-derived fungus showed pro-angiogenic activities in a zebrafish model [8]. We are also committed to find more marine natural products with angiogenesis related activity. In the present study, all isolated compounds were tested for the pro-angiogenic activities in a vatalanib (PTK787) induced vascular injury zebrafish model (Table S1). Compounds **5** and **7** (at concentrations of 30, 70 and 120 μg/mL) significantly promoted the angiogenesis, compounds **2** and **10** (70 and 120 μg/mL) also

had effects, and compounds **4** (120 μg/mL) exhibited moderate effects (Figure 4). Compared to compound **7**, compounds **8** and **9** were inactive with respect to pro-angiogenesis, indicating that phenolic hydroxyl group is necessary for pro-angiogenic activity. All compounds were also evaluated for anti-inflammatory effects in $CuSO_4$-induced zebrafish inflammation model (Table S1). Compound **11** (30, 70, and 120 μg/mL) displayed potent anti-inflammatory activity, and compounds **7**, **8**, and **10** (70, and 120 μg/mL) had moderate effects (Figure 5). Compound **7** showed better anti-inflammatory activity than **8**, while **9** was ineffective, suggesting the phenolic hydroxyl group and the epoxide oxygen are important in the anti-inflammatory activity. Meanwhile, compared to compound **11**, compounds **12**–**14** displayed no anti-inflammatory activity, indicating that both phenolic and alcohol-hydroxyl groups are necessary for anti-inflammatory activity. In addition, all compounds were tested for cytotoxicity against human liver carcinoma cells HepG2 by MTT method (Table S1) [20], and compound **6** exhibit cytotoxicity with an IC_{50} value of 30 μg/mL (Figure S1). The pro-angiogenic, anti-inflammatory activities in zebrafish and cytotoxicity against HepG2 cells of these compounds were reported here for the first time.

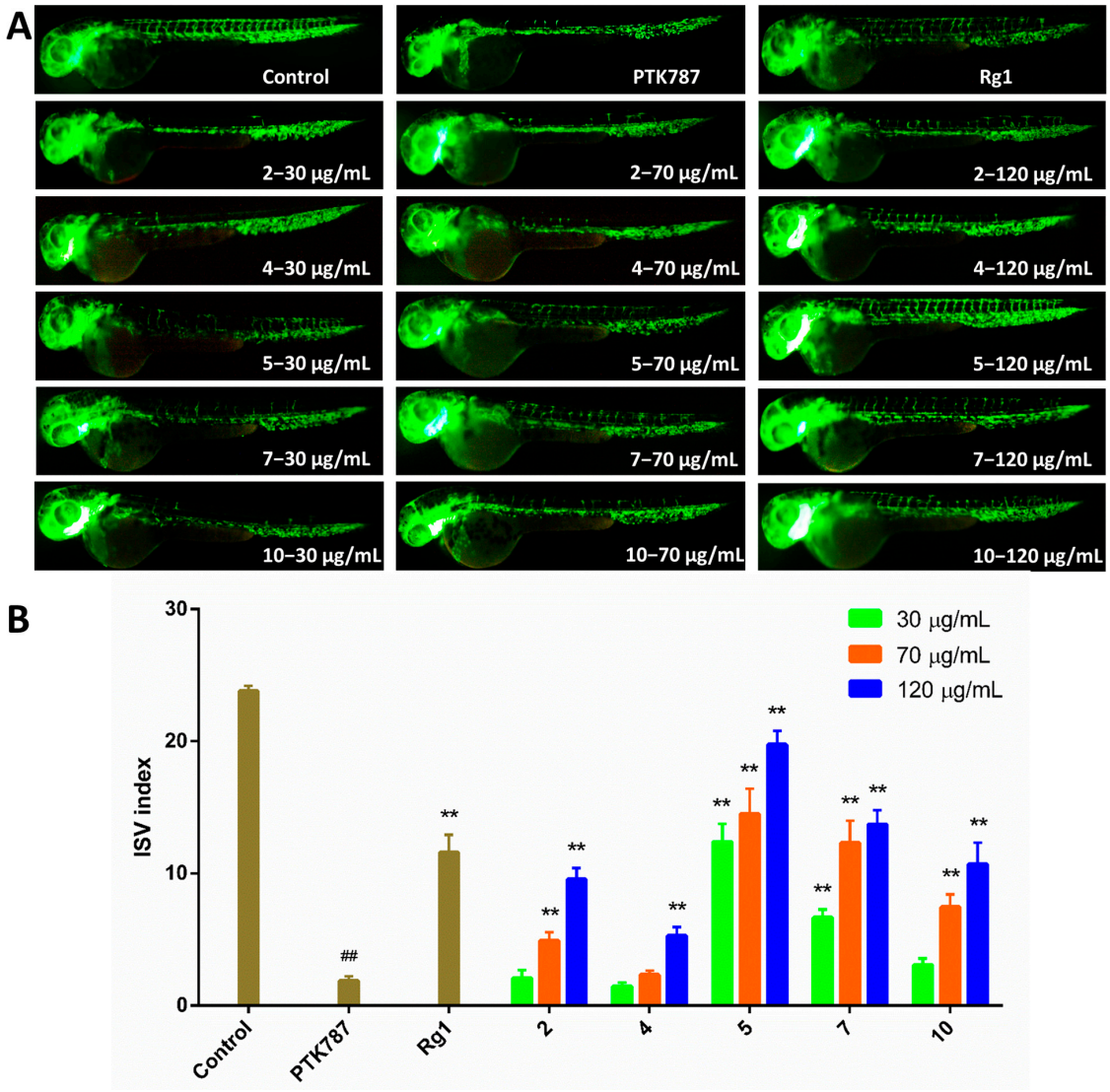

Figure 4. Results of pro-angiogenesis activities. (**A**) Typical images of intersomitic vessels (ISV) in transgenic fluorescent zebrafish (Tg (vegfr2: GFP)) treated with PTK787 and different concentrations (30, 70 and 120 μg/mL) of compounds **2**, **4**, **5**, **7**, and **10**, using ginsenoside Rg1 (120 μg/mL) as a positive control. (**B**) Quantitative analysis of the ISV index (number of intact vessels * 1+number of defective vessels * 0.5) in zebrafish treated with compounds **2**, **4**, **5**, **7**, and **10**. Data represented as mean ± SEM. $^{\#\#}$ $p < 0.01$ compared to the control group; ** $p < 0.01$ compared to the PTK787 group.

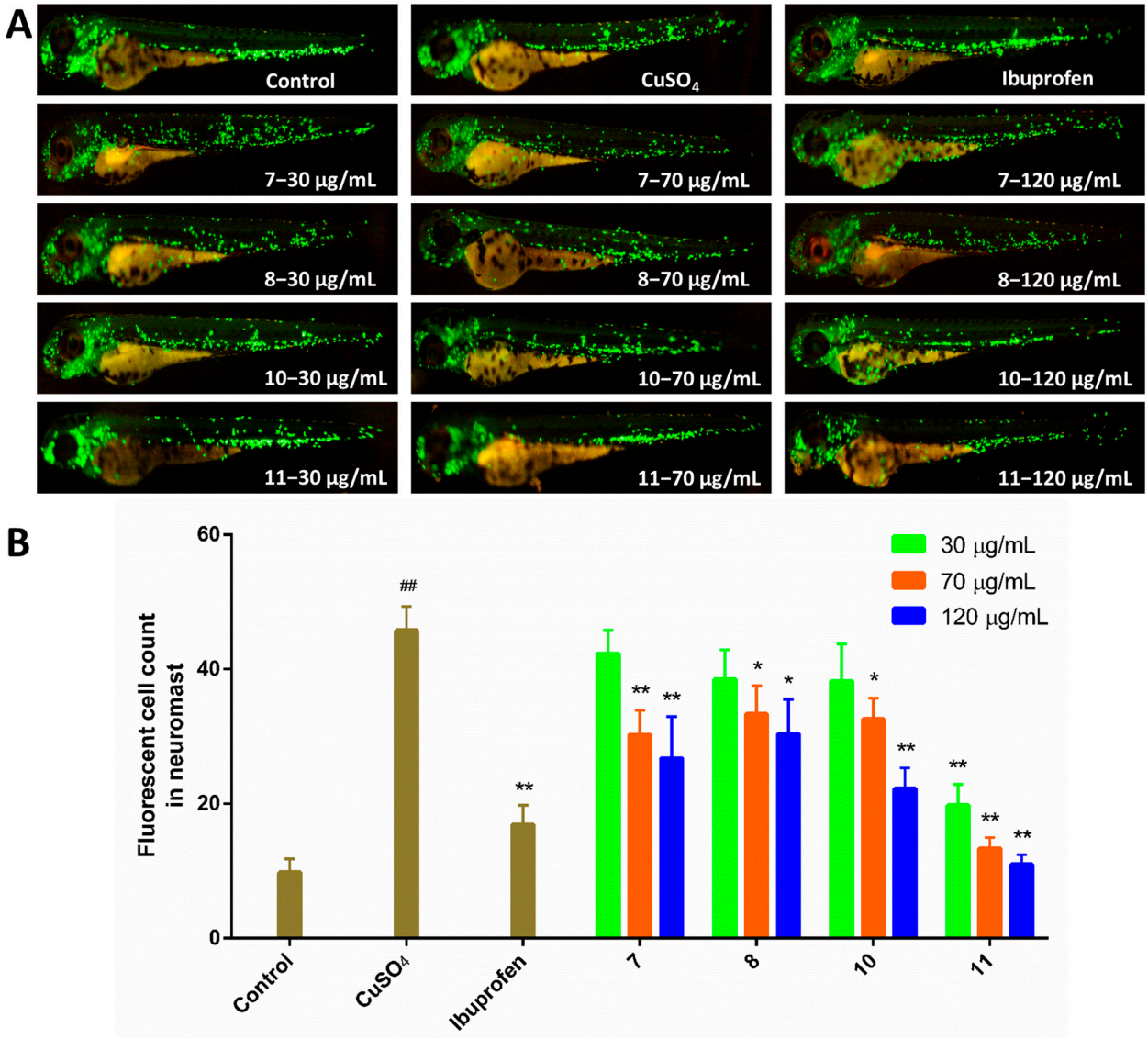

Figure 5. Results of anti-inflammatory activities. (**A**) Typical images on inflammatory sites in $CuSO_4$-induced transgenic macrophages fluorescent of compounds **7**, **8**, **10**, and **11**, using ibuprofen (10 μM) as a positive control. (**B**) Quantitative analysis of the number of fluorescent macrophages. The data are represented as the mean ± SEM. $^{\#\#}$ $p < 0.01$ compared to the control group; * $p < 0.05$ and ** $p < 0.01$ compared to the $CuSO_4$ group.

3. Materials and Methods

3.1. General Experimental Procedures

Optical rotations were measured on a JASCO P-2000 digital polarimeter (JASCO, Tokyo, Japan). UV spectra were performed on an Eppendorf BioSpectrometer Basic photometer. IR spectra were recorded on a JASCO FT/IR-4600 spectrometer in KBr discs. CD data were obtained on a JASCO J-810 spectropolarimeter. NMR spectra were collected using a JEOL JNM-ECP 600 spectrometer (JEOL, Tokyo, Japan). HRESIMS data were acquired on an Agilent 6210 ESI/TOF mass spectrometer (Agilent, Santa Clara, CA, USA). Analytical high performance liquid chromatography (HPLC) system (Waters, Milford, MA, USA) consisted of Waters e2695, UV Detector 2489, and software Empower using a C18 column (Diamonsil C18(2), 250 × 4.6 mm, 5 μM). Semipreparative HPLC was operated on the same system using a C18 column (Cosmosil 5C18-MS-II, 250 × 10 mm, 5 μM). Vacuum-liquid chromatography (VLC) used silica gel H (Qingdao Marine Chemical Factory, Qingdao, China). Thin layer chromatography (TLC) and column chromatography were performed

on plates pre-coated with silica gel GF254 (10–40 μm) and Sephadex LH-20 (GE Healthcare Biosciences, Uppsala, Sweden), respectively.

3.2. Fungal Material

The fungus Y32-2 was isolated from the seawater sample collected from a depth of about 30 m in the Indian Ocean (88°59′51″ E, 2°59′54″ S) in 2013. It was identified as *Aspergillus austroafricanus* (GenBank access No. MK267449) by rDNA amplification and sequence analysis of the ITS region. The producing strain was prepared on potato dextrose agar medium stored at 4 °C.

3.3. Fermentation and Extraction

The fungus was cultured in 500 mL Erlenmeyer flasks with fermentation media containing 80 g of rice and 120 mL of sea water at 28 °C for 40 days. The whole fermented material was extracted exhaustively with EtOAc. Then the EtOAc extract was dried under reduced pressure to obtain residue (30.1 g).

3.4. Purification and Identification

The EtOAc extract was subjected to silica gel chromatography with a vacuum liquid chromatography (VLC) column, using a stepwise gradient solvent system of petroleum ether (PE)-CH_2Cl_2 (7:3, 3:7 and 0:1), then of CH_2Cl_2-MeOH (99:1, 49:1, 19:1, 9:1, 4:1, 1:1, and 0:1) to obtain thirteen primary fractions (Fr.1–Fr.13). Fr.6–Fr.11 were individually subjected to Sephadex LH-20 column (120 × 2 cm) chromatography with CH_2Cl_2-MeOH (1:1) as mobile phase, and then fractions were purified separately by semipreparative HPLC column (Cosmosil 5C18-MS-II, 250 × 10 mm, 5 μM) using different gradients of MeOH in H_2O. Fr.6 (3.5 g) afforded **6** (70% MeOH-H_2O, *v*/*v*; t_R = 23.5 min; 12.4 mg), **8** (60% MeOH-H_2O, *v*/*v*; t_R = 20.5 min; 91.2 mg), **9** (60% MeOH-H_2O, *v*/*v*; t_R = 21.9 min; 12.8 mg), **13** (65% MeOH-H_2O, *v*/*v*; t_R = 25.9 min; 8.6 mg), **14** (60% MeOH-H_2O, *v*/*v*; t_R = 24.8 min; 4.7 mg). Fr.7 (2.7 g) afforded **4** (40% MeOH-H_2O, *v*/*v*; t_R = 18.5 min; 4.4 mg). Fr.8 (1.5 g) afforded **1** (70% MeOH-H_2O, *v*/*v*; t_R = 10.4 min, 14.4min; 6.5 mg), **7** (60% MeOH-H_2O, *v*/*v*; t_R = 16.9 min; 21.4 mg), **11** (60% MeOH-H_2O, *v*/*v*; t_R = 22.8 min; 5.6 mg), **12** (65% MeOH-H_2O, *v*/*v*; t_R = 26.0 min; 14.3 mg). Fr.9 (0.5 g) afforded **3** (65% MeOH-H_2O, *v*/*v*; t_R = 28.5 min; 4.5 mg), 10 (60% MeOH-H_2O, *v*/*v*; t_R = 22.5 min; 5.5 mg). Fr.10 (1.1 g) afforded **2** (60% MeOH-H_2O, *v*/*v*; t_R = 15.0 min; 5.1 mg). Fr.11 (1.3 g) afforded **5** (50% MeOH-H_2O, *v*/*v*; t_R = 14.5 min; 3.0 mg).

Di-6-hydroxydeoxybrevianamide E (**1**)*:* Yellow amorphous powder; $[\alpha]_D^{20}$ +24 (*c* 0.1, MeOH); UV (MeOH) λ_{max} 216, 299 nm; IR (KBr) ν_{max} 3460, 2973, 2925, 1667, 1440, 1306, 1192, 1108, 1001, 920, 809 cm^{-1}; ^1H and ^{13}C NMR data, see Table 1; HRESIMS *m*/*z* 731.3559 $[M - H]^-$ (calcd. for $C_{42}H_{48}N_6O_6$, 731.3557).

Dinotoamide J (**2**)*:* Yellow amorphous powder; $[\alpha]_D^{20}$ +22 (*c* 0.1, MeOH); UV (MeOH) λ_{max} 210, 226 and 295 nm; IR (KBr) ν_{max} 3447, 1646, 1442, 1186, 1105, 618 cm^{-1}; ^1H and ^{13}C NMR data, see Table 1; HRESIMS *m*/*z* 763.3440 $[M - H]^-$ (calcd. for $C_{42}H_{48}N_6O_8$, 763.3456).

Asperpteridinate A: Yellow amorphous powder; $[\alpha]_D^{20}$ +63 (*c* 0.1, MeOH); UV (MeOH) λ_{max} 218, 239, 300, 334 nm; ^1H and ^{13}C NMR data, see Table 2; IR (KBr) ν_{max} 3465, 1633, 1263, 1192, 1105, 615 cm^{-1}; HRESIMS *m*/*z* 465.1018 $[M + Na]^+$ (calcd. for $C_{20}H_{18}N_4O_8$, 465.1023).

3.5. ECD Computational Calculation

The conformational analyses were carried out by random searching in the Sybyl-X 2.0 using the MMFF94S force field with an energy cutoff of 5.0 kcal/mol [21]. Subsequently, the conformers were re-optimized using DFT at the PBE0-D3/def2-SVP level in MeOH using the polarizable conductor calculation model (SMD) by the GAUSSIAN 09 program [22]. The energies, oscillator strengths, and rotational strengths (velocity) of the first 30 electronic excitations were calculated using the TDDFT methodology at the CAM-B3LYP-D3/def2-SVP level in MeOH. The ECD spectra were simulated by the overlapping Gaussian function (half the bandwidth at 1/e peak height, sigma = 0.30 for all) [23]. To get the final spectra, the

simulated spectra of the conformers were averaged according to the Boltzmann distribution theory and their relative Gibbs free energy (ΔG).

3.6. Bioassay Protocols

3.6.1. Cell Culture and Cytotoxicity Assay

According to previous report [24], The HepG2 cells were cultured with DMEM medium, pH 7.0, supplemented with 10% FBS and 1% antibiotics (10,000 IU mL^{-1} of penicillin and 10 mg mL^{-1} of streptomycin), and the culture flasks were incubated under a humidified atmosphere of 37 °C and 5% CO_2. The cytotoxic activities of all compounds against HepG2 cells in vitro were determined by modified MTT assays as described previously [21]. Cells were seeded into a 96-well plate at a density 5×10^4 per well. After overnight incubation, the cells were treated with the chemicals for 24 h, and 10 μL MTT (5 mg/mL) was added to each well at 37 °C for 4 h, then 100 μL lysis buffer was added for the cell lysis. The OD value of each sample was detected at 560 nm using a microplate reader. The experiments were carried out in triplicate.

3.6.2. Zebrafish Maintenance

The zebrafish (*Danio rerio*) strains used in this assay were the AB wild-type, Tg (vegfr2-GFP) and Tg (zlyz-EGFP) transgenic lines [25,26]. They were maintained at 28.0 °C ± 0.5 °C in an automatic circulating tank system with light-dark cycle (14 h:10 h). The healthy adult zebrafish were placed in a breeding tank in the evening, and mated in the next morning. The fertilized eggs were collected, disinfected with methylene blue solution, and then raised in clean culture water including 5.0 mM NaCl, 0.17 mM KCl, 0.4 mM $CaCl_2$, and 0.16 mM $MgSO_4$ in a light-operated incubator.

3.6.3. Pro-Angiogenesis Assay

Vascular insufficiency in zebrafish was modeled by VEGFR tyrosine kinase inhibitor PTK787 to evaluate the effects of compounds on pro-angiogenesis according to previous report [8,26]. The healthy zebrafish larvae were separated into 24-well plates (ten embryos per well) in a 2 mL final volume of culture water at 24 h post fertilization (hpf). 0.2 μg/mL PTK787 was co-treated with each test compound (30, 70, 120 μg/mL) as test group. The control group was fresh culture water, the model group was 0.2 μg/mL PTK787, the positive drug group was 0.2 μg/mL PTK787 and 120 μg/mL ginsenoside Rg1. After 24 h incubation in a light-operated incubator at 28.0 °C ± 0.5 °C, the number of intersegmental blood vessels (ISVs) were captured by a fluorescent microscope (Olympus, SZX2-ILLTQ, Tokyo, Japan). Intact and defective vessels were counted separately and ISVs index was defined as follows: ISV index = number of intact vessels × 1 + number of defective vessels × 0.5 [27]. The zebrafish larvae without PTK787 in test group was used to evaluate the effects of compounds on anti-angiogenesis under the same conditions above described. All treatments were performed in triplicate.

3.6.4. Anti-Inflammatory Assay

The zebrafish inflammation model was induced by $CuSO_4$ to evaluate the effects of compounds on anti-inflammation [28]. In total, 72 hpf zebrafish larvae were distributed into 24-well plates (ten embryos per well) in a 2 mL final volume of culture water, and treated with different concentrations of each test compound (30, 70, 120 μg/mL) for 2 h as test group. Then $CuSO_4$ was added and incubated for 1 h. The control group was fresh culture water, the model group was 20 μM $CuSO_4$ and the positive drug group was 20 μM $CuSO_4$ and 10 μM ibuprofen. After 4 h incubation in a light-operated incubator at 28.0 °C ± 0.5 °C, the number of macrophages were imaged by a fluorescent microscope (Olympus, SZX2-ILLTQ, Tokyo, Japan). All treatments were performed in triplicate.

3.6.5. Statistical Analysis

Statistical analysis were processed by GraphPad Prism 6.0 software. All the experimental data were shown as mean ± SEM. The comparison between groups was performed by student's test. * $p < 0.05$ was considered as significant difference. ** $p < 0.01$ was a very significant difference.

4. Conclusions

To summarize, two new indole alkaloid dimers di-6-hydroxydeoxybrevianamide E (**1**), dinotoamide J (**2**) and one new pteridine alkaloid asperpteridinate A (**3**), together with eleven known compounds (**4**–**14**) were isolated from the marine-derived fungus *Aspergillus austroafricanus* Y32-2. Their structures including the absolute configurations were elucidated by various spectroscopic methods and ECD calculations. Among them, both di-6-hydroxydeoxybrevianamide E (**1**) and dinotoamide J (**2**) are homologous dimers that represent the novel examples of prenylated indole alkaloids. Asperpteridinate A is the first new alkaloid composed of pteridine and 1, 3-benzodioxole structures. All compounds were evaluated for pro-angiogenic, anti-inflammatory activities in the zebrafish models and cytotoxicity against HepG2 cells. Compounds **2**, **4**, **5**, **7**, and **10** exhibited pro-angiogenic activity, and compounds **7**, **8**, **10**, and **11** displayed anti-inflammatory activity in a dose-dependent manner, and compound **6** showed significant cytotoxicity against HepG2 cells with an IC_{50} value of 30 μg/mL. The results suggested that these compounds could be promising candidates for further pharmacologic and biosynthetic research.

Supplementary Materials: The following are available online at https://www.mdpi.com/1660-3397/19/2/98/s1, HRESIMS, 1D and 2D NMR spectra of all new compounds **1**–**3**, biological activities of all isolated compounds and dose–response curves of compound **6**, the atom coordinates and energies of new compounds **1**–**3**.

Author Contributions: P.L. performed isolation, structure determination and bioassays of the compounds and wrote the manuscript. M.Z. performed the fermentation of the fungus, extraction of the culture broths and isolation of the compounds. H.L. and R.W. performed the bioassays. H.H. carried out taxonomic identification of the fungus. X.L. and K.L. designed the study and revised the manuscript. H.C. collected the samples from the Indian Ocean and revised the manuscript. All authors have read and agreed to the published version of the manuscript.

Funding: This work was supported by the National Key R&D Program of China (2018YFC1707300), the Project funded by China Postdoctoral Science Foundation (2019M662418), the International Science and Technology Cooperation Program of Shandong Academy of Sciences (No. 2019GHZD10), the Foundation of State Key Laboratory of Biobased Material and Green Papermaking, Qilu University of Technology, Shandong Academy of Sciences (No. ZZ20190402), the National Natural Science Foundation of China (81602982), the Taishan Scholar Project from Shandong Province (ts20190950), and the China Ocean Mineral Resources Research and Development Association (DY135-R2-1-06 and DY135-B2-11).

Institutional Review Board Statement: The experiments were performed in accordance with standard ethical guidelines. The procedures were approved by the Ethics Committee of the Biology Institute of Shandong Academy of Science (SYXK LU 2020 0015).

Conflicts of Interest: The authors declare no conflict of interest.

References

1. Barbosa, F.; Pinto, E.; Kijjoa, A.; Pinto, M.; Sousa, E. Targeting antimicrobial drug resistance with marine natural products. *Int. J. Antimicrob. Agents* **2020**, *56*, 106005. [CrossRef]
2. Ma, H.G.; Liu, Q.; Zhu, G.L.; Liu, H.S.; Zhu, W.M. Marine natural products sourced from marine-derived *Penicillium* fungi. *J. Asian Nat. Prod. Res.* **2016**, *18*, 92–115. [CrossRef] [PubMed]
3. Lee, Y.M.; Kim, M.J.; Li, H.; Zhang, P.; Bao, B.; Lee, K.J.; Jung, J.H. Marine-derived *Aspergillus* species as a source of bioactive secondary metabolites. *Mar. Biotechnol.* **2013**, *15*, 499–519. [CrossRef] [PubMed]
4. Wang, K.W.; Ding, P. New bioactive metabolites from the marine-derived fungi *Aspergillus*. *Mini-Rev. Med. Chem.* **2018**, *18*, 1072–1094. [CrossRef]

5. Carbone, D.; Parrino, B.; Cascioferro, S.; Pecoraro, C.; Giovannetti, E.; Sarno, V.D.; Musella, S.; Auriemma, G.; Cirrincione, G.; Diana, P. 1,2,4-oxadiazole topsentin analogs with antiproliferative activity against pancreatic cancer cells, targeting GSK3β kinase. *ChemMedChem* **2021**, *16*, 537–554. [CrossRef] [PubMed]
6. Parrino, B.; Carbone, D.; Cascioferro, S.; Pecoraro, C.; Giovannetti, E.; Deng, D.; Sarno, V.D.; Musella, S.; Auriemma, G.; Cusimano, M.G.; et al. 1,2,4-oxadiazole topsentin analogs as staphylococcal biofilm inhibitors targeting the bacterial transpeptidase Sortase A. *Eur. J. Med. Chem.* **2020**, *209*, 112892. [CrossRef]
7. Li, P.; Fan, Y.; Chen, H.; Chao, Y.; Du, N.; Chen, J. Phenylquinolinones with antitumor activity from the Indian ocean-derived fungus *Aspergillus versicolor* Y31–2. *Chin. J. Oceanol. Limnol.* **2016**, *34*, 1072–1075. [CrossRef]
8. Fan, Y.; Li, P.; Chao, Y.; Chen, H.; Du, N.; He, Q.; Liu, K. Alkaloids with cardiovascular effects from the marine-derived fungus *Penicillium expansum* Y32. *Mar. Drugs* **2015**, *13*, 6489–6504. [CrossRef] [PubMed]
9. Zuleta, I.A.; Vitelli, M.L.; Baggio, R.; Garland, M.T.; Seldes, A.M.; Palermo, J.A. Novel pteridine alkaloids from the sponge *Clathria* sp. *Tetrahedron* **2002**, *58*, 4481–4486. [CrossRef]
10. Gubiani, J.R.; Teles, H.L.; Silva, G.H.; Young, M.C.M.; Pereira, J.O.; Bolzani, V.S.; Araujo, A.R. Cyclo-(trp-phe) diketopiperazines from the endophytic fungus *Aspergillus versicolor* isolated from *Piper aduncum*. *Quim. Nova* **2017**, *40*, 138–142. [CrossRef]
11. Yurchenk, A.N.; Smetanina, O.F.; Kalinovsky, A.I.; Pivkin, M.V.; Dmitrenok, P.S.; Kuznetsova, T.A. A new meroterpenoid from the marine fungus *Aspergillus versicolor* (Vuill.) Tirab. *Russ. Chem. Bull.* **2010**, *59*, 852–856. [CrossRef]
12. Hodge, R.P.; Harris, C.M.; Harris, T.M. Verrucofortine, a major metabolite of *Penicillium verrucosum* var. *cyclopium*, the fungus that produces the mycotoxin verrucosidin. *J. Nat. Prod.* **1988**, *51*, 66–73. [CrossRef]
13. Xin, Z.; Fang, Y.; Zhu, T.; Duan, L.; Gu, Q.; Zhu, W. Antitumor components from sponge-derived fungus *Penicillium auratiogriseum* Sp-19. *Chin. J. Mar. Drugs* **2006**, *25*, 1–6.
14. Feng, Y.; Han, J.; Zhang, Y.; Su, X.; Essmann, F.; Grond, S. Study on the alkaloids from two great white sharks antitumor components from sponge-derived fungus *Penicillium auratiogriseum* Sp-19. *Chin. J. Mar. Drugs* **2016**, *35*, 16–22.
15. Fujiia, Y.; Asahara, M.; Ichinoec, M.; Nakajima, H. Fungal melanin inhibitor and related compounds from *Penicillium decumbens*. *Phytochemistry* **2002**, *60*, 703–708. [CrossRef]
16. Ma, Y.; Qiao, K.; Kong, Y.; Li, M.; Guo, L.; Miao, Z.; Fan, C. A new isoquinolone alkaloid from an endophytic fungus R22 of *Nerium indicum*. *Nat. Prod. Res.* **2016**, *31*, 1258556. [CrossRef]
17. Tsukamoto, S.; Kato, H.; Samizo, M.; Nojiri, Y.; Ohnuki, H.; Hirota, H.; Ohta, T. Notoamides F-K, Prenylated indole alkaloids isolated from a marine-derived *Aspergillus* sp. *J. Nat. Prod.* **2008**, *71*, 2064–2067. [CrossRef]
18. Jennifer, M.F.; David, H.S.; Sachiko, T.; Robert, M.W. Studies on the biosynthesis of the notoamides: Synthesis of an isotopomer of 6-hydroxydeoxybrevianamide E and biosynthetic incorporation into notoamide. *J. Org. Chem.* **2011**, *76*, 5954–5958.
19. Li, Y.; Teng, Y.; Cheng, Y.; Wu, L. Study on the chemical constituents of mulberry. *J. Shenyang Pharm. Univ.* **2003**, *6*, 422–424.
20. Qi, J.; Liu, S.; Liu, W.; Cai, G.; Liao, G. Identification of UAP1L1 as tumor promotor in gastric cancer through regulation of CDK6. *Aging* **2020**, *12*, 6904–6927. [CrossRef]
21. *Sybyl Software*, version X 2.0; Tripos Associates Inc.: St. Louis, MO, USA, 2013.
22. Frisch, M.J.; Trucks, G.W.; Schlegel, H.B.; Scuseria, G.E.; Robb, M.A.; Cheeseman, J.R.; Scalmani, G.; Barone, V.; Mennucci, B.; Petersson, G.A.; et al. *Gaussian 09*; revision C 01; Gaussian, Inc.: Wallingford, CT, USA, 2009.
23. Stephens, P.J.; Harada, N. ECD cotton effect approximated by the Gaussian curve and other methods. *Chirality* **2010**, *22*, 229–233. [CrossRef] [PubMed]
24. Ottoni, C.A.; Maria, D.A.; Gonçalves, P.J.R.O.; Araújo, W.L.; Souza, A.O. Biogenic *Aspergillus tubingensis* silver nanoparticles' in vitro effects on human umbilical vein endothelial cells, normal human fibroblasts, HEPG2, and *Galleria mellonella*. *Toxicol. Res.* **2019**, *8*, 789801. [CrossRef] [PubMed]
25. Li, T.; Tang, X.; Luo, X.; Wang, Q.; Liu, K.; Zhang, Y.; Voogd, N.J.; Yang, J.; Li, P.; Li, G. Agelanemoechine, a dimeric bromopyrrole alkaloid with a pro-angiogenic effect from the south China sea sponge *Agelas nemoechinata*. *Org. Lett.* **2019**, *21*, 9483–9486. [CrossRef] [PubMed]
26. Wang, Q.; Tang, X.; Liu, H.; Luo, X.; Sung, P.J.; Li, P.; Li, G. Clavukoellians G–K, new nardosinane and aristolane sesquiterpenoids with angiogenesis promoting activity from the marine soft coral *Lemnalia* sp. *Mar. Drugs* **2020**, *18*, 171. [CrossRef]
27. Zhou, Z.Y.; Huan, L.Y.; Zhao, W.R.; Tang, N.; Jin, Y.; Tang, J.Y. *Spatholobi caulis* extracts promote angiogenesis in HUVECs in vitro and in zebrafish embryos in vivo via up-regulation of VEGFRs. *J. Ethnopharmacol.* **2017**, *200*, 74–83. [CrossRef]
28. Gui, Y.H.; Liu, L.; Wu, W.; Zhang, Y.; Jia, Z.L.; Shi, Y.P.; Kong, H.T.; Liu, K.C.; Jiao, W.H.; Lin, H.W. Discovery of nitrogenous sesquiterpene quinone derivatives from sponge *Dysidea septosa* with anti-inflammatory activity in vivo zebrafish model. *Bioorg. Chem.* **2020**, *94*, 103435. [CrossRef] [PubMed]